Electronic Properties of Graphite Nanotubules from Galvanomagnetic Effects

S. N. Song, X. K. Wang, R. P. H. Chang, and J. B. Ketterson
Materials Research Center, Northwestern University, Evanston, Illinois 60208
(Received 22 June 1993)

We have measured the magnetoresistance (MR) and Hall coefficient of state-of-the-art graphite nanotubule bundles. The apparent Hall coefficient is positive in the temperature and field ranges studied. At low temperatures, the conductivity σ shows two dimensional weak localization behavior and the MR is negative; above 60 K the MR is positive and σ increases approximately linearly with temperature, which is mainly due to an increase in the carrier concentration. The results show that a bundle of graphite nanotubules may best be described as a semimetal.

PACS numbers: 71.20.Hk, 72.15.Gd, 72.15.Rn

Recently the electronic properties of the newly discovered fullerene nanotubules (buckytubes) have been the subject of much attention [1]. A nanotubule may be visualized as a graphitic sheet rolled up in a helical fashion about the tube axis with a diameter ranging from a few to tens of Å. The electronic properties of this fascinating new structure are extremely interesting. Band structure calculations predict that graphite nanotubules can exhibit a striking variation in their electronic structure, ranging from metallic to semiconducting depending on the diameter of the tubule and the degree of helical arrangement [2]. Transport measurements are therefore required to distinguish which behavior occurs in practice. Since a transport measurement on a single nanotubule is not presently possible, we report results of magnetoresistance (MR) and Hall effect measurements on a state-of-the-art single graphite nanotubule bundle with a diameter of few tens of μm. The observed MR is positive above 60 K and can be described by a two band model with the majority carrier being p type. At low temperatures, the electronic conduction shows two dimensional (2D) weak localization (WL) behavior. The results imply that the buckytube bundles behave as a semimetal.

Fullerene nanotubules were prepared by an arc-discharge evaporation method as described elsewhere [3]. Structural characterization with transmission electron microscopy (TEM) [3] reveals that a single bundle consists of buckytubes, running parallel to one another with no graphite between them. The buckytubes have a wide range of diameters (20–300 Å with a mean diameter of about 100 Å) and tend to pack in an aligned, close-packed structure (see Fig. 1). Since the valence requirements of all atoms in a buckytube (with two sealed ends) are satisfied, the interaction among buckytubes should be van der Waals in nature. Therefore, it is energetically favorable for buckytubes packed closely together to form a "buckybundle."

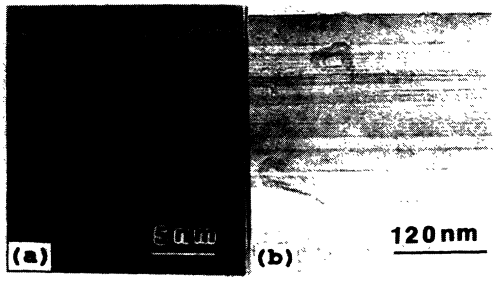

FIG. 1. TEM images of a buckytube (a) and a portion of a single buckybundle showing parallel buckytubes with an average diameter of about 100 Å (b).

The transport properties were measured using standard dc (for the Hall effect) and ac (for MR) four-terminal techniques. The I-V characteristic was measured to ensure Ohmic behavior so that no hot electron effects were present. The contact configuration is shown schematically by the inset in Fig. 2(a) [4]. The magnetic field was applied perpendicular to the tube axis. The measured MR and apparent Hall coefficient show essentially the same temperature and field dependence regardless of the samples used and the distance between the potential con-

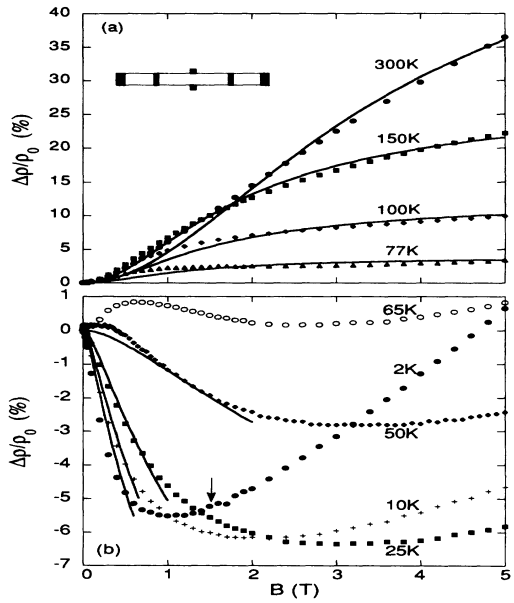

FIG. 2. (a),(b) The magnetic field dependence of the high and low temperature MR, respectively. The solid lines are calculated using Eq. (1) for (a) and Eq. (3) for (b). The inset shows a schematic of the contact configuration for the transport measurements.

0031-9007/94/72(5)/697(4)$06.00

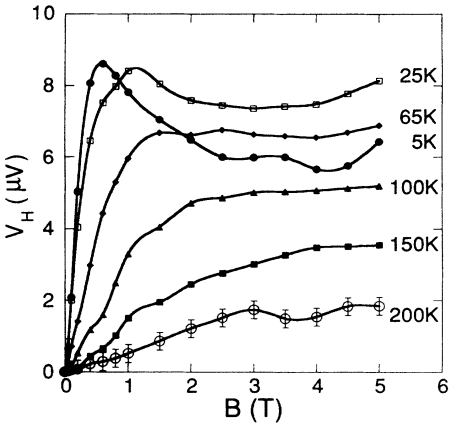

FIG. 3. Hall voltage vs magnetic field measured at different temperatures. The solid lines are drawn to guide the eye.

tacts, implying that the samples are homogeneous. For example, the residual resistivity ratios, $R(300\ \mathrm{K})/R(5\ \mathrm{K})$, measured on different single buckybundles agree with each other within 1%. In what follows we present the data taken on a single buckybundle having a diameter of 60 μm, the distance between the two potential contacts being 350 μm.

The transverse magnetoresistance data, ρ/ρ_0 [$\Delta\rho = \rho(B) - \rho_0$], measured at different temperatures are shown in Fig. 2. It is seen that above 60 K, the MR is positive; it increases with temperature and tends to saturate at a characteristic magnetic field which is smaller at lower temperatures. Based on a simple two band model, this means that unequal numbers of electrons and holes are present and that the difference in electron and hole concentrations decreases with increasing temperature [5]. At low temperatures, the MR is negative at low fields followed by an upturn at another characteristic field which depends on temperature. The observed Hall voltages are always positive. In Fig. 3 we show the measured Hall voltage V_H as a function of the applied field. The temperature dependence of the apparent Hall coefficient R_H, as determined by the slopes of the initial V_H vs B curves, is shown in Fig. 4 (left scale). The temperature dependence of the conductance (shown by the right scale in Fig. 4) cannot be described by thermal excitation (over an energy gap) or variable range hopping. Instead, above 60 K $\sigma(T)$ increases approximately linearly with temperature. At lower temperatures (below 20 K), as shown in Fig. 5, the zero-field resistance varies logarithmically with temperature signaling 2D WL behavior. Interestingly, the logarithmic temperature dependence extends to higher temperatures on applying a magnetic field. A least squares fit using the 1D WL expression for conduction (which assumes a power law temperature dependence of type $T^{-\nu}$) yields a very small exponent $\nu = 0.06$. Clearly the data cannot be described by 1D WL theory.

It is common to measure the magnetoresistance of carbon materials to gain information on their band structure and microtexture [6]. The MR is positive in well graphi-

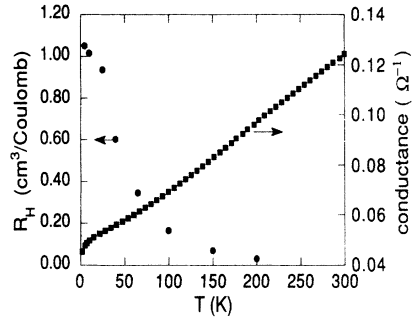

FIG. 4. The Hall coefficient (left scale) and conductance (right scale) vs temperature. R_H was determined using the measured sample dimensions without any correction.

tized samples. Negative MR has been observed in various kinds of poorly graphitized carbon materials [6,7]. Several models have been proposed to explain this unusual behavior. Among them, the model suggested by Yazawa [8] and extended by Bright [9] has received considerable attention. They argued that with increased magnetic field, the density of states and carrier density increase, resulting in a negative MR. However, our numerical calculations show that this model cannot describe our data. Our low temperature MR data has two striking features. First, as shown by the inset in Fig. 5, at low temperatures and low fields $\Delta\rho/\rho_0$ depends logarithmically on temperature while Bright's model predicts a $1/T$ dependence at low fields, Second, from Fig. 2(b) we see that the characteristic magnetic field at which the MR exhibits an upturn is smaller for lower temperatures. On the contrary, the transverse MR at different temperatures for the pyrocarbon exhibits quite a different behavior [10]: the upturn field decreases with temperature; with increasing temperature, the $\Delta\rho/\rho_0$ vs B curves shift upward regularly and there is no crossover between the curves measured at different temperatures. All these facts indicate that the negative MR has a different origin

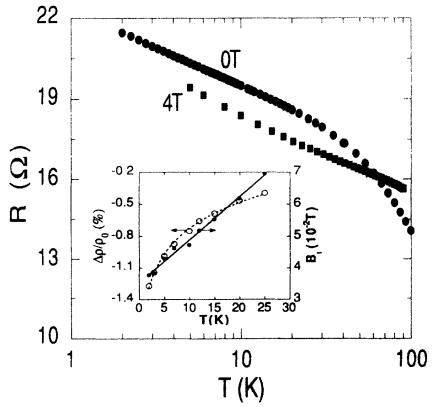

FIG. 5. The temperature dependence of the resistance in the low temperature region measured at two different applied magnetic fields. The inset shows the temperature dependence of the inelastic scattering field B_i (right scale) and the MR measured at 0.1 T (left scale). The solid line is a linear fit. The dashed line is calculated using $\Delta\rho/\rho_0 = 1.54 + 0.81 \ln(T)$.

for our buckytube samples as compared with the turbostratic graphite.

It is well known that in a 2D electronic system the observed increase in the resistance as the temperature decreases is due to the combined effects of weak localization and Coulomb interaction [11]. The destruction of the weak localization by a weak magnetic field leads to a negative MR which is apparent in very weak fields. Within the framework of WL and interaction theories, the effective dimensionality of the electronic system depends on several important length scales, i.e., the diffusion length $l_i=(D\tau_i)^{1/2}$, the magnetic length $l_H=(\phi_0/4\pi B)^{1/2}$, and the thermal length $l_T=(\hbar D/2\pi k_B T)^{1/2}$, where ϕ_0 is the flux quantum, D the diffusion constant, and τ_i is the inelastic relaxation time due to electron-electron and electron-phonon scattering. The criterion for 2D weak localization to occur is $l_i > d$ and $l_H > d$ and that for the 2D interaction effect is $l_T > d$ with d being the effective thickness of the system. Both l_i and l_T decrease with temperature. One then expects a 2D-3D crossover to occur at some elevated temperature. The WL theory has been used to interpret the observed negative MR in pregraphitic carbon fibers [12] and in fluorine-intercalated graphite fibers [13].

To deduce the transport coefficients, a knowledge of the effective dimensions of the tubes is required. The problem is complicated due to the fact that within one buckytube the graphite sheet rolls up with different diameters and within a single bundle the buckytubes have different diameters. In the following analysis, we will view the buckybundle as an effective medium characterized by an effective diameter, sheet resistance, etc. We examine the high temperature MR data first. In this temperature regime, the observed MR is a classical phenomenon. For a simple two band model, the MR is given by [14]

$$\frac{\Delta\rho}{\rho_0}=\frac{\sigma_e\sigma_p(\mu_e+\mu_p)^2B^2\cos^2\theta}{(\sigma_e+\sigma_p)^2+(\sigma_e\mu_p-\sigma_p\mu_e)^2B^2\cos^2\theta}, \quad (1)$$

where σ is the conductivity, μ is the mobility, and the subscripts e and p refer to electrons and holes, respectively; θ is the angle between the magnetic field and the graphite sheet normal. From Eq. (1), the measured MR is simply $\langle\Delta\rho/\rho_0\rangle$ and $\langle\ \rangle$ denotes an angular average.

Based on Eq. (1) the measured high temperature MR data were fitted using a least squares optimization procedure. The theoretical curves are presented in Fig. 2(a) as the solid lines. The fitting parameters are listed in Table I. It is found that to generate a better fit a hole mobility slightly smaller than the electron mobility is required. The Hall coefficient measurements reveal that the majority carrier is p type. From Table I we see that the ratio σ_p/σ_e decreases with increasing temperature, implying that as the temperature increases the Fermi level shifts closer to the conduction band. The increase in conductivity with temperature mainly arises from the increase in carrier concentration (see Fig. 4). The absence of an exponential or a variable range hopping type temperature dependence in the conductivity indicates that the system is semimetallic and that the hopping between the tubes within the bundle is not the dominant transport mechanism. Figures 3 and 4 show that initially V_H increases linearly with B and the corresponding slope (and hence the Hall coefficient) decreases with temperature. V_H tends to saturate at higher fields with the saturation field being higher at high temperatures. These behaviors are also consistent, qualitatively, with the two band model [14,15].

TABLE I. The parameters determined by fitting the high temperature MR data by Eq. (1).

T (K)	μ_p (m^2/Vs)	σ_p/σ_e	μ_p/μ_e
300	0.36	5.67	0.70
150	0.60	11.4	0.70
100	0.69	23.9	0.70
77	0.72	70.5	0.70

Since the ratio σ_p/σ_e increases with decreasing temperature, then according to Eq. (1), when $\sigma_p/\sigma_e \to \infty$, $\Delta\rho/\rho_0 \to 0$. Therefore, at low temperature, the MR is mainly a quantum phenomenon, i.e., it arises from the WL and interaction effects [16]. In the 2D WL regime, the sheet resistance, $R_\square$, at zero field is given by [11]

$$\Delta R_\square/R_\square = -R_\square(e^2/2\pi^2\hbar)C\ln(T/T_0), \quad (2)$$

where T_0 is a characteristic temperature and the coefficient C characterizes the strength of weak localization and interaction. The logarithmic fit in Fig. 5 yields that $CR_\square = 5.5\ \mathrm{k\Omega/\square}$. For the 2D WL case, the complete expression for the transverse MR is given in Refs. [17,18]. The theory of the interaction effect predicts a positive, isotropic MR.

At low fields, the MR arising from the interaction effect is very small compared to the MR due to localization. Note spin-orbit scattering results in an antilocalization effect leading to a positive MR, which was not observed at low temperatures. Furthermore, we expect that the spin scattering effect is negligible because of the ultrahigh purity of the material used in sample preparation. Therefore, to a good approximation the contribution of spin-orbit and spin scatterings may be ignored. The negative MR due to weak localization is then given by

$$\frac{\Delta R_\square(B\cos\theta,T)}{R_\square(0,T)}=-R_\square(0,T)\frac{e^2}{2\pi^2\hbar}\left\{\psi\left(\frac{1}{2}+\frac{B_i}{B\cos\theta}\right)-\ln\left[\frac{B_i}{B\cos\theta}\right]\right\}, \quad (3)$$

where $B_i=\hbar/4eD\tau_i$ and $\tau_i \propto T^{-p}$ is assumed. The low field MR data can be fitted [using Eq. (3) averaged over angle θ] to deduce the quantities $B_i(T)$ and $R_\square$. The solid lines in Fig. 2(b) are the theoretical curves based on Eq. (3).

The fitting yields $R_\square = 5.95$ k$\Omega/\square$, which depends on temperature only weakly. The deduced inelastic scattering field B_i is shown in the inset of Fig. 5 as a function of temperature. The solid line is calculated using $B_i(T) = (0.035 + 0.0014T)$ T. Since B_i depends on T linearly, $p = 1$. Therefore the dominant scattering mechanism at low temperatures is carrier-carrier scattering. If spin scattering is taken into account, we obtain from the fitting the spin scattering field $B_S \sim 40$ G.

The upturn in the MR at high fields may be due to the interaction effect which is significant when the splitting between the spin-up and spin-down bands is much greater than the thermal energy $k_B T$, i.e., when $h = g\mu_B B/k_B T \gg 1$ (g is the g factor and μ_B the Bohr magneton). Since the available field range does not warrant a clear differentiation between the two effects, we will not fit the high-field MR data; instead, we simply mark the field at which $h = 1$ for $T = 2$ K [shown as an arrow in Fig. 2(b)].

To estimate the dimensionality we need to know the diffusion constant D and resistivity ρ which are not well defined quantities. However, we may estimate their order of magnitude. The measured resistivity is 0.0065 Ω cm at 300 K and 0.016 Ω cm at 5 K. We believe the true resistivity along the tube axis should be much smaller due to the following factors: (i) the filling factor of the nanotubules in the bundle is less than 1, (ii) the inside of the tubes is hollow, and (iii) the system is anisotropic. If we take $d \approx 100$ Å (as determined by our TEM observations), and $R_\square = \rho/d = 5.95$ k$\Omega/\square$, then $\rho \sim 5.9 \times 10^{-3}$ Ω cm at 5 K. Since $\mu \approx e\tau_0/m^*$, using the μ values in Table I and assuming $m^* \sim 0.012 m_0$ (m_0 is the electron mass) [12], we estimate the elastic relaxation time $\tau_0 \sim 10^{-14}$ sec. Ignoring the Hall scattering factor and using $R_H = 1/ne$, the carrier density $n \approx 10^{18}/\text{cm}^3$ at low temperatures, yielding a typical Fermi velocity $v_F \sim 10^8$ cm/s (see Fig. 4). Therefore, $D = v_F^2 \tau_0/2 \approx 50$ cm^2/s and $k_F l \sim 5$. The fitting yield $B_i = 0.043$ T at 5 K and 0.28 T at 50 K, corresponding to $l_i \sim 600$ and 200 Å, respectively. We estimate that $l_T \sim 350$ Å at 5 K and 110 Å at 50 K. Therefore, at low temperatures the system is in the 2D WL-interaction regime. Above 50 K, the relevant length scales (l_i and l_T) are comparable to the average diameter of the buckytubes. Hence a 2D-3D crossover should occur in the vicinity of this temperature.

The above analysis indicates that the buckytubes show 2D WL behavior at low temperatures. In disordered turbostratic graphite, the graphite microcrystallites orient randomly. However, in fullerene tubules the disorder is weak and possibly stems from the helical structure (with a varying helical pitch) or from the topological defects proposed by Saito, Dresselhaus, and Dresselhaus [19]. The absence of the spin-orbit scattering effect and weak spin scattering imply the impurity levels in the samples are very low. Our transport measurements indicate that the buckytube is neither a large-gap nor a medium-gap semiconductor. At low temperatures, the electronic structure is essentially two dimensional in character.

We are grateful to A. Patashinski and V. Dravid for useful discussion. This work was supported, in part, by the NSF under Grant No. DMR91-20521.

[1] S. Iijima, Nature (London) **354**, 56 (1991).

[2] N. Hamada, S. Sawada, and A. Oshiyama, Phys. Rev. Lett. **68**, 1579 (1992); J. W. Mintmire, B. I. Dunlap, and D. C. White, Phys. Rev. Lett. **68**, 631 (1992); R. Saito *et al.*, Appl. Phys. Lett. **60**, 2204 (1992); K. Harigaza, Phys. Rev. B **45**, 12071 (1992).

[3] X. K. Wang *et al.*, Appl. Phys. Lett. **62**, 1881 (1993).

[4] Gold wires were attached to the sample with Du Pont conductor composition. The current and potential contacts covered, respectively, the entire end and the semicircumferences of the bundle to ensure a uniform current distribution and equipotential. The Hall arms had a diameter less than 40 μm. To eliminate the effects of the thermal electromotive force and any Hall-probe misalignment, the directions of the current and magnetic field were separately reversed, and the four measured voltages were averaged to yield the apparent Hall voltage.

[5] J. Callaway, *Quantum Theory of the Solids* (Academic, New York, 1976), p. 614.

[6] I. L. Spain, in *Chemistry and Physics of Carbon*, edited by P. L. Walker, Jr. and P. A. Thrower (Marcel Dekker, New York, 1981), Vol. 16.

[7] H. H. Sample, L. J. Neuringer, and L. G. Rubin, Rev. Sci. Instrum. **45**, 64 (1974).

[8] K. Yazawa, J. Phys. Soc. Jpn. **26**, 1407 (1969).

[9] A. A. Bright, Phys. Rev. B **20**, 5142 (1979).

[10] P. Delhaes, P. de Kepper, and M. Uhlrich, Philos. Mag. **29**, 1301 (1974).

[11] P. A. Lee and T. V. Ramakrishnan, Rev. Mod. Phys. **57**, 287 (1985).

[12] V. Bayot *et al.*, Phys. Rev. B **40**, 3514 (1989).

[13] S. L. di Vittorio *et al.*, Phys. Rev. B **43**, 12304 (1991); **43**, 1313 (1991).

[14] K. Noto and T. Tsuzuku, Jpn. J. Appl. Phys. **14**, 46 (1975).

[15] Strictly speaking, the measured Hall coefficient can only be defined as some transport coefficient relating to the Hall effect. Because of the sample geometry, both in-plane and out-of-plane components, which assume different angular dependence, are present.

[16] This has been demonstrated in boronated and neutron irradiated graphites, see Y. Hishiyama *et al.*, Carbon **9**, 367 (1971). The field dependence of the negative MR shown in Fig. 2 is in disarray with what would be expected from a hopping mechanism, see N. F. Mott and F. A. Davis, *Electronic Processes in Non-Crystalline Materials* (Clarendon, Oxford, 1979), p. 242.

[17] G. Bergmann, Phys. Rep. **107**, 1 (1984); S. Hikami, A. I. Larkin, and Y. Nagaoka, Prog. Theor. Phys. **63**, 707 (1980).

[18] D. E. Beutler and N. Giordano, Phys. Rev. B **38**, 8 (1988).

[19] R. Saito, G. Dresselhaus, and M. S. Dresselhaus, Chem. Phys. Lett. **195**, 537 (1992).

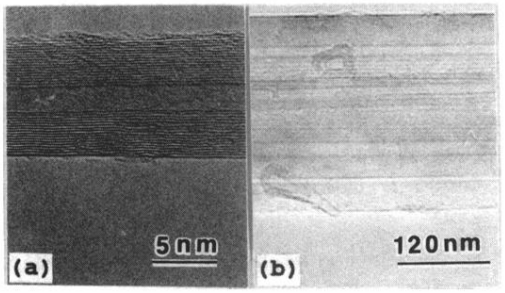

FIG. 1. TEM images of a buckytube (a) and a portion of a single buckybundle showing parallel buckytubes with an average diameter of about 100 Å (b).